ISSN 1674-1056
http://cpb.iphy.ac.cn
http://iopscience.iop.org/cpb
中国物理 B
Chinese Physics
中国物理 Chinese Physics B

Low temperature magnetism in the rare-earth perovskite $GdScO_3$

Jie-Ming Sheng(盛洁明), Xu-Cai Kan(阚绪材), Han Ge(葛晗), Pei-Qian Yuan(袁培骞), Lei Zhang(张磊), Nan Zhao(赵南), Zong-Mei Song(宋宗美), Yuan-Yin Yao(姚远寅), Ji-Ning Tang(唐霁宁), Shan-Min Wang(王善民), Ming-Liang Tian(田明亮), Xin Tong(童欣), Liu-Suo Wu(吴留锁)
Citation: Chin. Phys. B . 2020, 29(5): 057503 . **doi:** 10.1088/1674-1056/ab8200
Journal homepage: http://cpb.iphy.ac.cn; http://iopscience.iop.org/cpb

What follows is a list of articles you may be interested in

Mn-based permanent magnets

Jinbo Yang(杨金波), Wenyun Yang(杨文云), Zhuyin Shao(邵珠印), Dong Liang(梁栋), Hui Zhao(赵辉), Yuanhua Xia(夏元华), Yunbo Yang(杨云波)
Chin. Phys. B . 2018, 27(11): 117503 . **doi:** 10.1088/1674-1056/27/11/117503

Influence of Tb on easy magnetization direction and magnetostriction of $PrFe_{1.9}$ alloy

Chang-Xuan He(何昌璇), Yan-Mei Tang(唐妍梅), Xiang Li(李翔), Yun He(何云), Cai-Yan Lu(陆彩燕), Ze-Ping Guo(郭泽平)
Chin. Phys. B . 2019, 28(11): 117501 . **doi:** 10.1088/1674-1056/ab47f6

Magnetism manipulation in ferromagnetic/ferroelectric heterostructures by electric field induced strain

Xiaobin Guo(郭晓斌), Dong Li(李栋), Li Xi(席力)
Chin. Phys. B . 2018, 27(9): 097506 . **doi:** 10.1088/1674-1056/27/9/097506

Micromagnetism simulation on effects of soft phase size on $Nd_2Fe_{14}B/\alpha$–Fe nanocomposite magnet with soft phase imbedded in hard phase

Yu-Qing Li(李玉卿), Ming Yue(岳明), Yi Peng(彭懿), Hong-Guo Zhang(张红国)
Chin. Phys. B . 2018, 27(8): 087502 . **doi:** 10.1088/1674-1056/27/8/087502

Magnetic properties of misch-metal partially substituted Nd-Fe-B magnets sintered by dual alloy method

Jie-Fu Xiong(熊杰夫), Rong-Xiang Shang(商荣翔), Yan-Li Liu(刘艳丽), Xin Zhao(赵鑫), Wen-Liang Zuo(左文亮), Feng-Xia Hu(胡凤霞), Ji-Rong Sun(孙继荣), Tong-Yun Zhao(赵同云), Ren-Jie Chen(陈仁杰), Bao-Gen Shen(沈保根)
Chin. Phys. B . 2018, 27(7): 077504 . **doi:** 10.1088/1674-1056/27/7/077504

RAPID COMMUNICATION

Low temperature magnetism in the rare-earth perovskite $GdScO_3$*

Jie-Ming Sheng(盛洁明)[1,2,3,†], Xu-Cai Kan(阚绪材)[4,†], Han Ge(葛晗)[1], Pei-Qian Yuan(袁培骞)[1], Lei Zhang(张磊)[1], Nan Zhao(赵南)[1], Zong-Mei Song(宋宗美)[1], Yuan-Yin Yao(姚远寅)[1], Ji-Ning Tang(唐霁宁)[1], Shan-Min Wang(王善民)[1], Ming-Liang Tian(田明亮)[4,5], Xin Tong(童欣)[2,3,‡], and Liu-Suo Wu(吴留锁)[1,§]

[1] *Department of Physics, Southern University of Science and Technology, Shenzhen* 518055, *China*
[2] *Institute of High Energy Physics, Chinese Academy of Sciences (CAS), Beijing* 100049, *China*
[3] *Spallation Neutron Source Science Center, Dongguan* 523803, *China*
[4] *School of Physics and Materials Science, Anhui University, Hefei* 230601, *China*
[5] *High Magnetic Field Laboratory, Chinese Academy of Science (CAS), Hefei* 230031, *China*

(Received 2 January 2020; revised manuscript received 16 March 2020; accepted manuscript online 23 March 2020)

The magnetic phase diagram of rare-earth perovskite compound, $GdScO_3$, has been investigated by magnetization and heat capacity. The system undergoes an antiferromagnetic phase transition at $T_N = 2.6$ K, with an easy axis of magnetization along the a axis. The magnetization measurements show that it exists a spin-flop transition around 0.3 T for the applied field along the a axis. The critical magnetic field for the antiferromagnetic-to-paramagnetic transition is near 3.2 T when temperature approaches zero. By scaling susceptibilities, we presume this point ($B = 3.2$ T, $T = 0$ K) might be a field-induced quantum critical point and the magnetic critical fluctuations can even be felt above T_N.

Keywords: rare-earth perovskite, magnetization, spin-flop transition, quantum critical point

PACS: 75.47.Lx, 75.50.Ee, 75.40.–S, 75.40.Cx **DOI:** 10.1088/1674-1056/ab8200

1. Introduction

The family of rare-earth perovskite scandates $R ScO_3$ ($R =$ rare earth) have attracted continued attention due to great variety of physical properties and potential applications. For example, the Ising-like antiferromagnet,[1] the giant magnetocaloric effect,[2,3] and the promising candidate materials for the replacement of SiO_2 in silicon MOSFETs because of the large optical band gaps, high dielectric constants, and chemical stabilities.[4–9] In addition, the $R ScO_3$ compounds with different lattice parameters have also been exploited to serve as substrates for engineering of highly strained ferroelectric and multiferroic thin films. The biaxial strain due to lattice mismatch between substrates and thin films can dramatically alter the properties of epitaxial films.[10] For instance, the $SrTiO_3$ thin film exhibits a strain-induced ferroelectricity at room temperature when it is grown on $DyScO_3$ substrate, compared with the paraelectric behavior of bulk unstrained $SrTiO_3$.[11] The compressively strained $BaTiO_3$ thin films grown on $DyScO_3$ and $GdScO_3$ substrates can also produce larger ferroelectric (FE) polarization and higher FE transition temperature.[12]

Apart from the effect of strain, the intrinsic properties of $R ScO_3$ substrates may also play important effect on the properties of thin films. For example, the magnetic properties of $R ScO_3$ should be took into account when they are used as substrates for magnetic oxide thin films.[13] However, due to the low magnetic ordering temperatures of $R ScO_3$, normally only a few Kelvin degrees,[13–15] the magnetic effects from the substrates to the magnetic thin films are usually neglected and have not been the subject of detailed investigation. However, some of this series compounds still exist strong magnetic correlation well above the magnetic transition temperature, which cannot be ignored even at dozens of Kelvin degrees, such as the short range magnetic order discovered in $DyScO_3$ at 30 K.[1] Actually, it was argued that these strong fluctuations are enhanced by the one dimensionality of the rare earth magnetic spin chains. Indeed, the quantum critical Tomonaga–Luttinger liquid behavior has been reported in $YbAlO_3$,[16] and the strong orbital couplings and crystal field effects was claimed to be crucial for the unexpected low dimensionality behaviors.[1,16,17]

On the other side, for $GdScO_3$, with the electron configuration of Gd^{3+} is $4f^7$ and $L = 0$, no spin–orbit coupling is expected. Thus following the arguments in previous studies,[1,16,17] the low-temperature magnetism of $GdScO_3$ should behave very different, comparing with $DyScO_3$ and $YbAlO_3$. Despite that $GdScO_3$ has been reported as a giant magnetocaloric system with an antiferromagnetic (AFM)

*The work at SUSTech was supported by the National Natural Science Foundation of China (Grant No. 11974157). Part of this work was also supported by the National Natural Science Foundation of China (Grant No. 11875265), the Scientific Instrument Developing Project of the Chinese Academy of Sciences (^{3}He-based neutron polarization devices), and the Institute of High Energy Physics, the Chinese Academy of Sciences. Kan X C and Tian M L were supported by the National Natural Science Foundation of China (Grant No. 51802002).

†These authors contributed equally to this work.
‡Corresponding author. E-mail: tongx@ihep.ac.cn
§Corresponding author. E-mail: wuls@sustech.edu.cn

© 2020 Chinese Physical Society and IOP Publishing Ltd

transition, $T_N = 2.6$ K,[3] the details of the magnetic phase diagram and Gd–Gd interactions still remained poorly understood. Moreover, the studying of the Gd–Gd interactions in $GdScO_3$ may also be very helpful to understand the complex magnetism in $GdFeO_3$ and $GdMnO_3$.[18,19]

2. Experimental details

High-quality single crystals of $GdScO_3$ used here are commercially available.[12,20] Magnetization measurements were performed using two magnetometers for different temperature ranges: (i) commercial vibration sample magnetometer Quantum Design Magnetic Property Measurement System (MPMS-VSM) for the high-temperature measurements $T = 1.8$ K–300 K; (ii) MPMS-3 with ^{3}He insert for the temperatures $T = 0.5$ K–1.5 K. Heat capacity measurements were performed on the Physical Property Measurement System (PPMS) in the temperature range 1.8 K–300 K.

3. Results and analysis

As shown in Fig. 1(a), $GdScO_3$ crystallizes in a distorted orthorhombic perovskite structure with $a = 5.4862$ Å, $b = 5.7499$ Å, and $c = 7.9345$ Å in the *Pbnm* (No. 62) space group at room temperature.[21] Gd^{3+} ions are located between 8 distorted ScO_6 octahedrons. Due to the distortion, the point symmetry of the Gd site is decreased from O_h in the ideal cubic $Pm\bar{3}m$ structure to C_s, which is only one mirror plane normal to the c axis, in the orthorhombic structure. Figure 1(b) illustrates the T dependence of specific heat of $GdScO_3$ single crystal. A sharp anomaly appears near 2.6 K indicating a magnetic transition similar to $GdAlO_3$.[22] The temperature evolution of the magnetic susceptibility $\chi(T)$ with an applied magnetic field of 0.3 T along the three principle crystal axis is shown in Fig. 1(c). The anomalies observed around 2.6 K confirm the AFM phase transition. The AFM order is mainly from a competition between exchange interactions and dipolar magnetic interactions for the neighbouring Gd^{3+} ions.[23] The Néel temperature $T_N = 2.6$ K of $GdScO_3$ is lower than the isostructural $GdAlO_3$ ($T_N = 3.98$ K).[22] This may be due to Sc^{3+} ion has larger ionic radius than Al^{3+} ion, which leads to larger distance between the neighbouring Gd^{3+} ions and produces smaller magnetic interactions. Above T_N, the susceptibilities $\chi(T)$ along the three principle crystal axis almost overlap together except the small T region near T_N, which indicates $GdScO_3$ only exists very weak anisotropy. This is consistent with the $S = 7/2$, $L = 0$ electron configuration of Gd^{3+} ion. Below T_N, it is seen that the susceptibility for the field parallel to axes b and c varies very little with temperature, whereas that when the field is parallel to the a axis decreases steeply (see the inset of Fig. 1(c)). Unlike the magnetic A_x structure preferred by the direct dipole–dipole interaction only, the magnetization with easy axis along a is consistent with the AF magnetic structure (G_x) as observed in $GdAlO_3$,[22] where the exchange interaction between the large Gd^{3+} $S = 7/2$ spins in ab plane is dominant. This is very different from the cases of $DyScO_3$ and $YbAlO_3$.[1,16,17] Figure 1(d) displays the inverse susceptibility plotted against the temperature for magnetic field applied along the c axis. Fits of $1/\chi_c$ for the paramagnetic (PM) region (15 K $< T <$ 300 K) to a Curie–Weiss law yield Curie temperature θ_{CW} of -4.85 K and effective magnetic moment μ_{eff} of 7.45 μ_B/Gd. The negative value in θ_{CW} confirms AFM interactions between the neighboring Gd^{3+} ions. The large $\mu_{eff} = 7.45$ μ_B/Gd compared with the theoretical value of 7.94 μ_B assuming a spin of 7/2 for the Gd^{3+} ions.

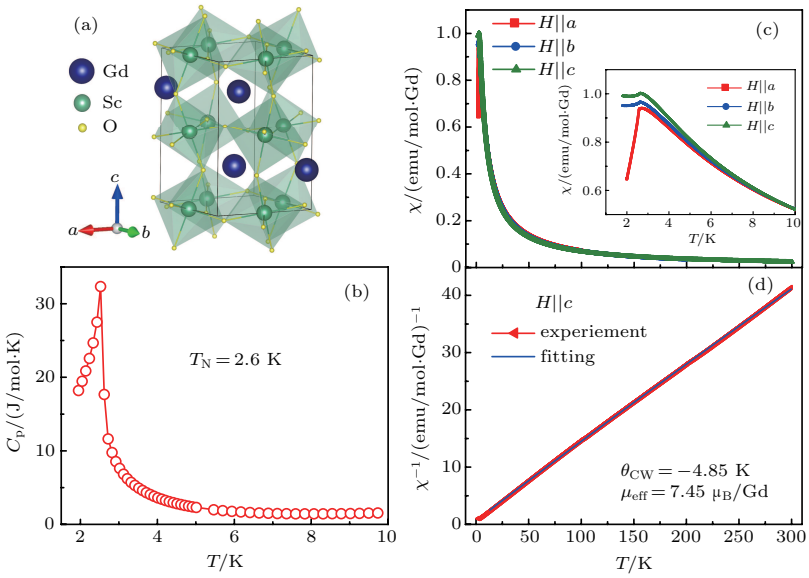


Fig. 1. (a) Crystal structure of $GdScO_3$ in space group *Pbnm*, where a Gd^{3+} ion is surrounded by eight distorted ScO_6 octahedrons. (b) T dependence of specific heat $C_p(T)$. (c) T dependence of magnetic susceptibility $\chi(T)$ in an applied magnetic field of 0.3 T parallel to the a, b, and c axes, respectively. The inset: $\chi(T)$ near the AFM transition. (d) T dependence of inverse magnetic susceptibility $1/\chi(T)$ with 0.3-T magnetic field along the c axis. The blue solid line is the fit using the Curie–Weiss law above the transition temperature.

Figure 2(a) illustrates the isothermal magnetizations of $GdScO_3$ as a function of applied field along the a axis ranging from 1.0 K to 5.0 K. The magnetizations closely approach to saturation around $M = 6.5$ μ_B/Gd above 5 T, which is consistent with the reported saturated moment of Gd^{3+} ion.[22] An enlarged view of the low-field region of $M(B)$ curves is shown in Fig. 2(b). All of the magnetization curves for $T < T_N$ show an abrupt change around the field between 0.2 T and 0.45 T. This suggests the occurrence of a spin flop (SF) type transition, similar as the transition reported in $GdAlO_3$,[22] where the spin direction of two sublattice Gd^{3+} ions suddenly turn perpendicular to the easy axis direction. This is due to the lower Zeeman energy of Gd^{3+} spins for the applied field along the easy axis until reaching the critical field of SF transition B_{c1}. In addition, the observed hysteresis loop shown in the inset of Fig. 2(a) indicates the SF transition is a subsequent field-induced first-order transition. With increasing of temperature, B_{c1} also increases. This behavior is slightly different with $GdAlO_3$, in which the critical field is almost independent of T.[22] Above B_{c1}, the magnetizations increase linearly with the field, and break off at a point which gives an AFM-to-PM critical field B_{c2}. The T-dependent magnetization of $GdScO_3$ with field applied along the a axis is shown in Fig. 2(c). Two anomalies are observed at 1.97 K and 2.55 K for $B = 0.35$ T, which correspond SF transition and AFM-to-PM phase transition, respectively. For the former, as the applied magnetic field increases, the phase transition T also increases, while the latter has the opposite trend (see the dash lines in Fig. 2(c)). Figure 2(d) shows the contour plot of magnetic phase diagram for applied field along the a axis. The intensity corresponds to the susceptibility $\chi = dM/dB$. Below T_N, the critical field of SF transition divides the phase diagram into two regions. At the low-field region, $GdScO_3$ is an antiferrromagnet, in which the spin directions of Gd^{3+} ions are dominantly aligned in the a axis, and each Gd^{3+} ion in one sublattice might be surrounded by six nearest neighbours Gd^{3+} ions with opposite moments direction belonging to the other sublattice like $GdAlO_3$[23] (the magnetic structure of $GdScO_3$ should be confirmed by neutron diffraction). Above B_{c1}, the moments turn perpendicular to the a axis due to the lower ground energy. A further increase of field rotates the spins continuously, until an AFM–PM critical field B_{c2} is reached where all the moments are polarized along the applied field.

The measurement of isothermal magnetizations of $GdScO_3$ with applied field along the b and c axes from 1.8 K to 3.0 K is shown in Figs. 3(a) and 3(c), respectively. Both the saturation moments and critical fields along the two axes are very similar with the a axis, which is consistent with the S-state of Gd^{3+} ions. In addition, since the spins direction of Gd^{3+} ions are dominantly along the a axis, there is no SF transition occurred when the field along the two axes. Figures 3(b) and 3(d) illustrate the magnetic phase diagram for field parallel to the b and c axes, respectively. With the increasing field, the AFM arrangement of spins of two-sublattice Gd^{3+} ions are gradually polarised, forming a PM magnetic state.

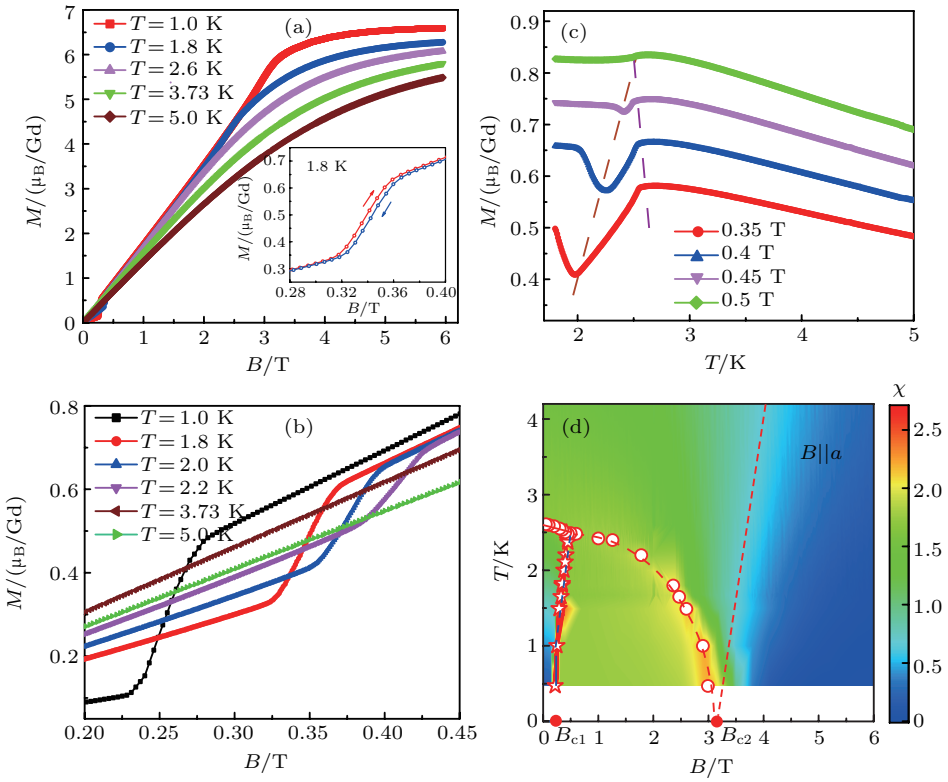


Fig. 2. (a) Field dependence of magnetization M of $GdScO_3$, measured at different T, with field along the a axis. (b) The magnetization discontinuity at several T corresponds the SF phase transition. (c) T dependence of magnetization M of $GdScO_3$ measured at several fields along the a axis. (d) The contour plot of the magnetic phase diagram of $GdScO_3$ with applied field along the a axis.

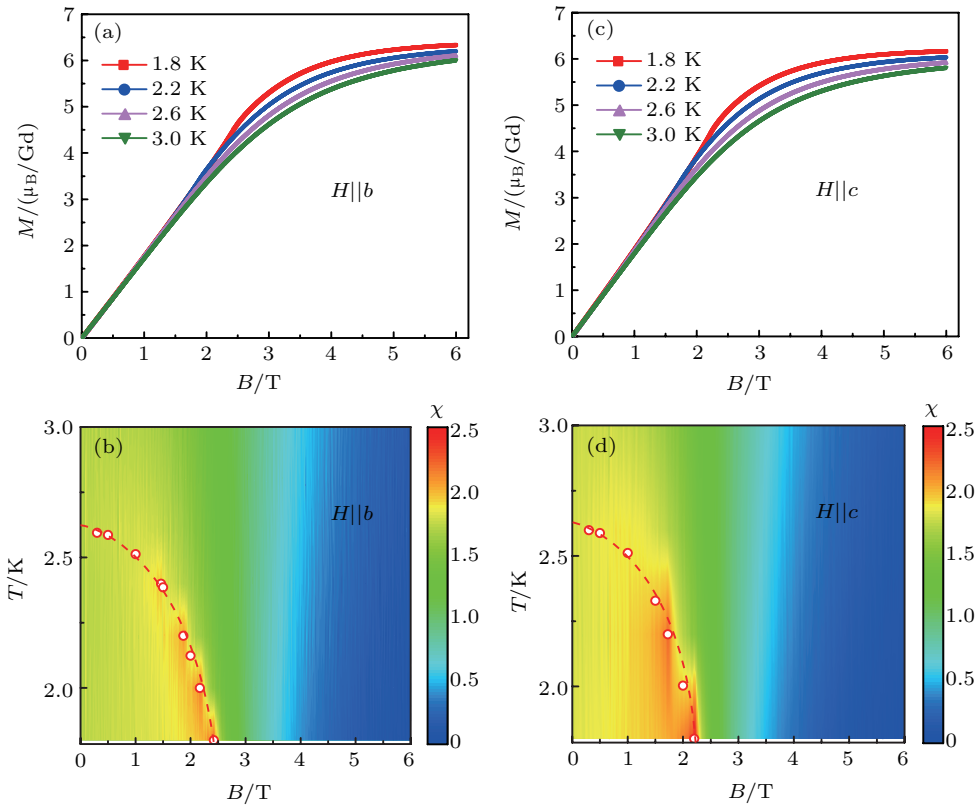


Fig. 3. (a) and (c) Field dependence of magnetization M of $GdScO_3$, measured at different T, with field along the b and c axes. (b) and (d) The contour plot of the magnetic phase diagram of $GdScO_3$ with applied field along the b and c axes. The AFM to PM phase boundary is given by the red open circles.

It usually believed that the AFM phase will directly enter into trivial PM phase in $GdScO_3$ with the applied field increased. However, since the AFM–PM transition is of second order and the transition temperature is gradually suppressed by the applied field, it might be existed a quantum critical field B_{c2} at 0 K, where the AFM state transforms into the PM state. Around the QCP, the magnetic fluctuations are quantum mechanical in nature, which can exhibit scale invariance in both space and time. Unlike classical critical points, where the critical fluctuations are limited to a narrow region around the phase transition, the influence of the QCP can be felt over a wide range of temperatures above the QCP, so the effect of quantum criticality is felt without ever reaching 0 K. Figure 4(a) illustrates the field-dependence of the magnetic susceptibilities $\chi = \mathrm{d}M/\mathrm{d}B$ measured below and above T_N. Around the QCP, susceptibilities with different T can be scaled as

$$\frac{\mathrm{d}M}{\mathrm{d}B} \cdot T^{2/\nu z-(d+z)/z} = f\left(\frac{\tilde{B}}{T^{1/\nu z}}\right), \tag{1}$$

where d is the spatial dimension, ν is the scaling exponent related to the magnetic field, z is the dynamical exponent, and $\tilde{B} = B - B_{c2}$ ($B_{c2} \simeq 3.2$ T at 0 K). The relationship between d, ν, and z can be obtained by scaling the susceptibility curves as shown in Fig. 4(a) and minimizing the deviation:

$$\nu z = 1, \tag{2}$$

$$2 - \nu(d+z) = 0.08. \tag{3}$$

The equations give

$$\nu z = 1, \quad d \approx z, \tag{4}$$

yielding the interesting result that the spatial dimension d is approximately equal to the dynamical exponent z in $GdScO_3$. The susceptibility curves scales well for temperatures from 1.0 K to 4.2 K and the scaling behaviors observed are consistent with a two dimensional QCP, where $d = 2$, $z \approx 2$, and $\nu \approx 1/2$. This is not very surprising.

As previous discussed, in $GdScO_3$, the orbital contribution ($L = 0$) is absent, and the magnetic ground states of Gd^{3+} are isotropic eight-degenerated $S = 7/2$ states. Due to the large spin values of $S = 7/2$, the in plane exchange interactions of the form $JS \cdot S$ are greatly enhanced, and become dominant in $GdScO_3$ and $GdAlO_3$.[23]

On the other hand, although sharing the same crystal structure, the situations in $YbAlO_3$ and $DyScO_3$ are completely different. Due to the large orbital contributions, the degenerated spin states of $YbAlO_3$ and $DyScO_3$ are lifted by the crystal field effect, and the ground states are well separated Kramer doublets. These doublet ground states could be treated as effective spin $S = 1/2$, which turns out to be crucial for observed unconventional one dimensional physics in $YbAlO_3$ and $DyScO_3$ and related systems.[16,17]

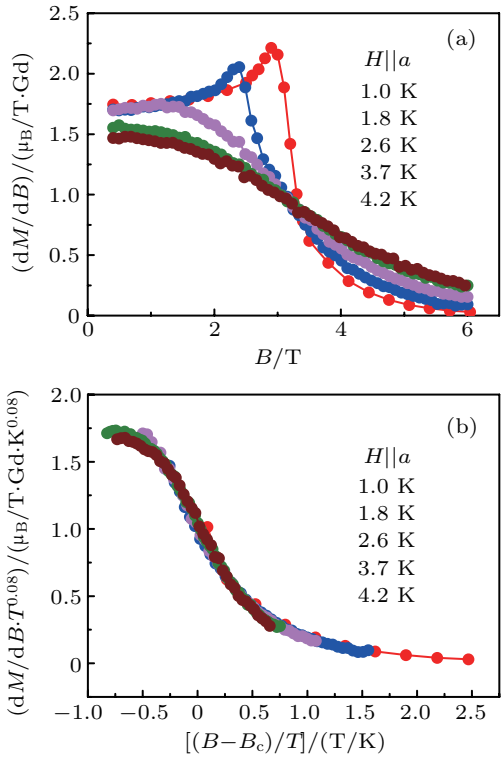


Fig. 4. (a) Field dependencies of the magnetic susceptibility $\chi = \mathrm{d}M/\mathrm{d}B$ from 1.0 K to 4.2 K with field along a axis. (b) Critical scaling of the magnetic susceptibility in panel (a).

4. Conclusion

In summary, we investigated the magnetism and heat capacity of single crystal $GdScO_3$ at low temperatures. $GdScO_3$ is an uniaxial antiferromagnet with the easy axis of magnetization along the a axis. The Néel temperature is found to be 2.6 K. The magnetization measurements show it exists an SF phase transition when the applied field along the a axis. The field-temperature phase diagrams for B along the three principle crystal axes are established. By scaling the magnetic susceptibilities, we demonstrate there might be a quantum critical point (QCP) at $B = 3.2$ T and $T = 0$ K corresponding to the AFM-to-PM phase transition. Compared to the one-dimensional physics observed in $YbAlO_3$ and $DyScO_3$, the magnetic structure and the critical scaling indicate that the in-plane exchange interactions are more important in $GdScO_3$. It is found that quantum critical like fluctuations affect the physical properties over a large temperature and field area in $GdScO_3$, and additional caution may need be paid at low temperatures, when it was treated as a simple PM substrates for the epitaxial growth of magnetic thin films.

References

[1] Wu L S, Nikitin S E, Frontzek M, Kolesnikov A I, Ehlers G, Lumsden M D, Shaykhutdinov K A, Guo E J, Savici A T and Gai Z 2017 *Phys. Rev. B* **96** 144407

[2] Wu Y D, Qin Y L, Ma X H, Li R W, Wei Y Y and Zi Z F 2019 *J. Alloys Compd.* **777** 673

[3] Jia J H, Ke Y J, Zhang X X, Wang J F, Su L, Wu Y D and Xia Z C 2019 *J. Alloys Compd.* **803** 992

[4] Schlom D G and Haeni J H 2002 *MRS Bull.* **27** 198

[5] Lim S G, Kriventsov S, Jackson T N, Haeni J H, Schlom D G, Balbashov A M, Uecker R, Reiche P, Freeouf J L and Lucovsky G 2002 *J. Appl. Phys.* **91** 4500

[6] Lucovsky G, Zhang Y, Whitten J L, Schlom D G and Freeouf J L 2004 *Microelectronic Engineering* **72** 288

[7] Lucovsky G, Hong J G, Fulton C C, Zou Y, Nemanich R J, Ade H, Scholm D G and Freeouf J L 2004 *Physica Status Solidi* **241** 2221

[8] Delugas P, Fiorentini V, Filippetti A and Pourtois G 2007 *Phys. Rev. B* **75** 115126

[9] Christen H M, Jellison G E Jr, Ohkubo I, Huang S, Reeves M E, Cicerrella E, Freeouf J L, Jia Y and Schlom D G 2006 *Appl. Phys. Lett.* **88** 262906

[10] Schlom D G, Chen L Q, Eom C B, Rabe K M, Streiffer S K and Triscone J M 2007 *Ann. Rev. Mater. Res.* **37** 589

[11] Haeni J H, Irvin P, Chang W, Uecker R, Reiche P, Li Y L, Choudhury S, Tian W, Hawley M E, Craigo B, *et al.* 2004 *Nature* **430** 758

[12] Choi K J, Biegalski M, Li Y L, Sharan A, Schubert J, Uecker R, Reiche P, Chen Y B, Pan X Q, Gopalan V, *et al.* 2004 *Science* **306** 1005

[13] Ke X, Adamo C, Schlom D G, Bernhagen M, Uecker R and Schiffer P 2009 *Appl. Phys. Lett.* **94** 152503

[14] Plaza I, Palacios E, Bartolomé J, Rosenkranz S, Ritter C and Furrer A 1997 *Physica B* **234** 635

[15] Raekers M, Kuepper K, Bartkowski S, Prinz M, Postnikov A V, Potzger K, Zhou S, Arulraj A, Stüßer N, Uecker R, *et al.* 2009 *Phys. Rev. B* **79** 125114

[16] Wu L S, Nikitin S E, Wang Z, Zhu W, Batista C D, Tsvelik A M, Samarakoon A M, Tennant D A, Brando M, Vasylechko L, *et al.* 2019 *Nat. Commun.* **10** 698

[17] Wu L S, Nikitin S E, Brando M, Vasylechko L, Ehlers G, Frontzek M, Savici A T, Sala G, Christianson A D, Lumsden M D, *et al.* 2019 *Phys. Rev. B* **99** 195117

[18] Tokura Y, Seki S and Nagaosa N 2014 *Rep. Prog. Phys.* **77** 076501

[19] Kimura T, Lawes G, Goto T, Tokura Y and Ramirez A P 2005 *Phys. Rev. B* **71** 224425

[20] Schubert J, Trithaveesak O, Petraru A, Jia C L, Uecker R, Reiche P and Schlom D G 2003 *Appl. Phys. Lett.* **82** 3460

[21] Liferovich R P and Mitchell R H 2004 *J. Solid State Chem.* **177** 2188

[22] Blazey K W and Rohrer H 1968 *Phys. Rev.* **173** 574

[23] Quezel S, Mignod J R and Tcheou F 1982 *Solid State Commun.* **42** 103